

# High-Field Multinuclear Magnetic Resonance Studies of Hexamethyldisilane in Liquid and Solid Phases

D. W. Aksnes<sup>†,a</sup> and L. Kimtys<sup>b</sup>

<sup>a</sup>Department of Chemistry, University of Bergen, N-5007 Bergen, Norway and <sup>b</sup>Department of Physics, Vilnius University, Vilnius 2734, Lithuania

Aksnes, D. W. and Kimtys, L., 1995. High-Field Multinuclear Magnetic Resonance Studies of Hexamethyldisilane in Liquid and Solid Phases. – Acta Chem. Scand. 49: 722–727 © Acta Chemica Scandinavica 1995.

<sup>1</sup>H, <sup>2</sup>H, <sup>13</sup>C and <sup>29</sup>Si NMR linewidths, self-diffusion coefficients and spin–lattice relaxation times ( $T_1$ ) have been measured at high field (4.7 and/or 9.4 T) in the liquid and solid phases of hexamethyldisilane. The abrupt decrease in the <sup>1</sup>H and <sup>13</sup>C linewidths at the solid II→solid I transition point is attributed to the onset of overall molecular tumbling, whereas the additional line-narrowing occurring in solid I is caused by molecular self-diffusion. The average time between diffusional jumps is  $1.7 \times 10^{-7}$  s, whereas the directly measured self-diffusion coefficient is  $7.0 \times 10^{-12}$  m<sup>2</sup> s<sup>-1</sup>, both parameters being obtained at the melting point. A thorough analysis of the  $T_1$  data for all phases is reported. The activation energies of the reorientational motions are accidentally nearly the same for both solid phases (6.9–7.1 kJ mol<sup>-1</sup>), although the spin–lattice relaxation is governed by internal reorientations about the C–Si or Si–Si bonds in the ordered phase and overall molecular tumbling in the disordered phase. The similar rotational correlation times, obtained from the <sup>1</sup>H, <sup>2</sup>H and <sup>13</sup>C  $T_1$ -values at the melting point (1.4–2.4 ps), indicate that the relaxation in solid I is dominated by the overall tumbling motion.

Many spherical molecules, e.g. adamantane and *tert*-butyl compounds, are known to exist in an orientationally disordered (plastic) crystalline phase of high symmetry, usually cubic, immediately below the melting point.<sup>1,2</sup> There are also many examples of less symmetrical molecules which exhibit orientationally disordered phases, e.g. the ditetrahedral molecules pivalic acid, hexamethylethane and hexamethyldisilane.<sup>1,2</sup> These elongated molecules also form cubic high-temperature phases with very considerable disorder. At lower temperatures transitions usually occur to one or more ordered phases of lower symmetry, where the molecules become more closely packed and the crystals exhibit normal mechanical properties. The different solid phases are usually designated I, II, III in order of decreasing temperature. In the ordered phase anisotropic molecular motions take place, whereas in the disordered and liquid phases overall molecular tumbling and translational diffusion occur.

In this paper we present the results of high-field <sup>1</sup>H, <sup>2</sup>H, <sup>13</sup>C and <sup>29</sup>Si linewidth, relaxation and self-diffusion measurements of the liquid and solid phases of hexamethyldisilane (HMDS). This compound exhibits a disordered phase between the phase transition at 221.7 K and the melting point at 287.7 K.<sup>3</sup> X-Ray studies have established that the disordered phase (solid I) is body-

centred cubic with two molecules per unit cell and a lattice constant ( $a$ ) of 0.847 nm at 273 K<sup>3</sup> and 0.843 nm at 225 K.<sup>4</sup> The entropy of fusion is low compared with the entropy of transition:  $\Delta S_f = 1.25 R$  and  $\Delta S_t = 5.25 R$ .<sup>3</sup>

In an early <sup>1</sup>H linewidth study<sup>5</sup> on HMDS it was concluded, on the basis of the motionally averaged second moment, that the methyl reorientation ( $C_3$  motion) is occurring at a faster rate than the molecular reorientation about the Si–Si axis ( $C_3'$  motion) in solid II. Two later low-field <sup>1</sup>H relaxation studies ( $T_1$  and  $T_{1\rho}$ ) are based on the same assumption.<sup>6,7</sup> However, neither <sup>1</sup>H second-moment<sup>8</sup> nor relaxation-time<sup>9</sup> measurements can distinguish between  $C_3$  and  $C_3'$  motions of a C(CH<sub>3</sub>)<sub>3</sub> or Si(CH<sub>3</sub>)<sub>3</sub> group with tetrahedral geometry since the dominating intra-CH<sub>3</sub> contributions will be the same for both motions. In the case of <sup>2</sup>H, <sup>13</sup>C and <sup>29</sup>Si NMR, however, different situations occur for  $C_3$  and  $C_3'$  motions, thus making a unique assignment of these motions possible in favourable situations.<sup>8,10</sup> Another complicating factor when interpreting the low-field <sup>1</sup>H NMR data is the unknown contribution from intermolecular interactions. This contribution is negligible for <sup>1</sup>H and <sup>13</sup>C at high field and <sup>2</sup>H at all fields.

Previous NMR relaxation and radio-tracer studies<sup>5–7,12,13</sup> on HMDS have shown that the translational diffusion rate is relatively high in the disordered phase. However, there is a significant difference in the self-dif-

<sup>†</sup> To whom correspondence should be addressed.

fusion coefficients ( $D$ ) obtained from the two techniques. In this context it should be mentioned that radio-tracer and pulsed field-gradient (PFG) methods give  $D$  directly, whereas the evaluation of  $D$  from  $T_{1\rho}$  relies on a model framework for the molecular dynamics. Further, considerable discrepancies exist in the reported activation energies of the rotational and translational motions of HMDS.<sup>5-7,12</sup> It therefore seemed to be a reasonable approach to study the dynamics of the liquid and solid phases of HMDS in greater detail using high-field multi-nuclear NMR.

## Experimental

Hexamethyldisilane (HMDS), obtained from Aldrich, was transferred into the inner tube (3 mm o.d.) of a special 5 mm coaxial Wilmad insert, degassed by four freeze-pump-thaw cycles and sealed under vacuum. The outer 5 mm o.d. tube contained a small amount of deuteriochloroform or DMSO- $d_6$  which served as external  $^2\text{H}$  lock signal source for the lower or higher temperatures, respectively. Two samples were also prepared in 5 mm and 10 mm o.d. NMR tubes using the same procedure as above.

The  $^1\text{H}$  and  $^{13}\text{C}$  measurements were carried out on Bruker AC 200 F and AM 400 WB spectrometers at 200.13 and 400.13 MHz ( $^1\text{H}$ ) and at 50.32 and 100.62 MHz ( $^{13}\text{C}$ ). Both spectrometers were equipped with a Z-shielded 5 mm probe-head. The 3 mm sample was used for all  $^1\text{H}$  relaxation and self-diffusion measurements. The  $^{13}\text{C}$  relaxation and self-diffusion measurements were carried out on the 3 mm sample for the liquid phase and the 5 mm sample for the solid phases. The  $^2\text{H}$  and  $^{29}\text{Si}$  relaxation measurements were performed on the Bruker AM 400 WB spectrometer at 61.42 and 79.50 MHz, respectively, using the 5 mm sample for the liquid phase and the 10 mm sample for the disordered (solid I) phase.  $^1\text{H}$  composite pulse decoupling with a Waltz-16 sequence was used when measuring the  $^{13}\text{C}$ ,  $^2\text{H}$  and  $^{29}\text{Si}$  spectra. All measurements on the 5 and 10 mm samples were done without an NMR lock.

The  $90^\circ$  transmitter pulses were carefully calibrated for all nuclei, samples and temperatures (ca. 7–26  $\mu\text{s}$ ). The field gradients were generated by a Bruker BGR gradient unit. The gradient pulses were shaped and the strengths calibrated ( $G \leq 0.86 \text{ T m}^{-1}$ ), according to procedures described by the Bruker company.<sup>13</sup> The measured gradient strengths ( $G$ ) agreed within experimental error with the values obtained indirectly from the reported self-diffusion constant of water.<sup>14</sup> The sample temperature was regulated and stabilized to within  $\pm 0.5 \text{ K}$  by means of a Bruker B-VT 1000 temperature-control unit. The heating air flow rate was  $10 \text{ l min}^{-1}$ .

The  $T_1$  times were measured by standard inversion-recovery<sup>15</sup> ( $180^\circ - \tau - 90^\circ - T$ )<sub>n</sub>, typically using 16 values of  $\tau$  and the recycle delay  $T \geq 5T_1$ . The diffusion coefficients were measured using the well established pulsed

field-gradient (PFG) technique<sup>15</sup> ( $T - 90^\circ - \tau - \delta - \tau - 180^\circ - \tau - \delta - \tau$ )<sub>n</sub>, where  $T \geq 5T_1$  and  $\delta$  is the length of the gradient pulses. By keeping the total time between the RF pulses  $\Delta = 2\tau + \delta$  constant the signal height of the Fourier transformed echo may be written  $A = \text{const} \times \exp(-\gamma^2 G^2 D \delta^2 (\Delta - \delta/3))$ . The *const* term contains a factor  $\exp(-2\Delta/T_2)$  which severely attenuates the measured echo for short spin-spin relaxation times  $T_2$ . The experiments were performed with  $\Delta = 100$  and 8 ms for the liquid and solid I phases, respectively. The gradient pulse length ( $\delta$ ) was decremented in 1 ms steps between 40 ms and 1 ms. The estimated errors of  $T$  and  $D$  are 3 and 6%, respectively.

## Results and discussion

**NMR linewidths and self-diffusion.** The  $^1\text{H}$ ,  $^2\text{H}$  and  $^{13}\text{C}$  linewidths,  $\Delta\nu_{1/2}$  (full width at half-height) of solid HMDS are shown in Fig. 1. The measurements were made by both cooling and warming the sample, and no hysteresis was observed. The linewidth of the  $^1\text{H}$  resonance in solid II (ca. 18 kHz) is in accordance with the value found for *tert*-butyl groups narrowed by  $\text{C}_3 + \text{C}_3'$  reorientations.<sup>1,2</sup>  $^1\text{H}$  composite pulse decoupling reduces the  $^{13}\text{C}$  resonance in solid II to some extent. The relatively sharp NMR resonances in solid I show that the intramolecular dipolar and quadrupolar interactions and most of the intermolecular dipolar interactions are averaged out by the overall tumbling motion in this phase. The remaining heteronuclear  $^1\text{H}$ - $^{13}\text{C}$  dipolar interactions are removed by proton decoupling. The observed line-narrowing of the  $^1\text{H}$  resonance (34–3900 Hz) is thus caused by molecular self-diffusion with activation energy  $42 \text{ kJ mol}^{-1}$  (*vide infra*). By contrast, the observed line-narrowing of the  $^2\text{H}$  signal (6–45 Hz) is attributed to rotational aver-

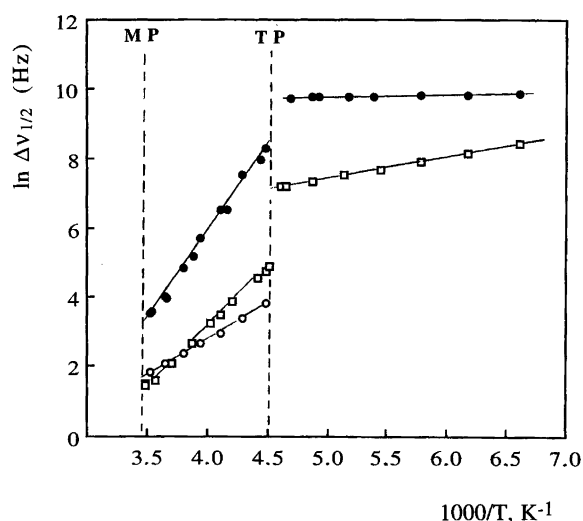


Fig. 1. NMR linewidths of HMDS versus reciprocal temperature for the  $^1\text{H}$  (●),  $^{13}\text{C}$  (□) and  $^2\text{H}$  (○) resonances measured at 400.13, 100.62 and 61.42 MHz, respectively.

aging of the intramolecular electric quadrupole interaction by the overall tumbling motion.

It is estimated that the intermolecular  $^{13}\text{C}$ - $^{13}\text{C}$  and  $^{13}\text{C}$ - $^{29}\text{Si}$  dipolar interactions give rise to a rotationally averaged  $^{13}\text{C}$  linewidth of approximately 32 Hz for a body-centered cubic structure with a lattice constant  $a$  of 0.847 nm.<sup>10,16</sup> The observed  $^{13}\text{C}$  linewidth is 32 Hz at 243 K but appreciably wider below, and narrower above, this temperature (4–130 Hz). The relatively broad lines and long  $T_1$  times at low-temperatures might indicate a slightly ordered structure. The additional line-narrowing which occurs in the high-temperature region of solid I is attributed to molecular self-diffusion. The  $E_a$  value (28 kJ mol<sup>-1</sup>) therefore largely reflects the translational diffusion process.

The  $^1\text{H}$  linewidth data of HMDS were converted to  $T_2$  values, assuming a Lorentzian line-shape, according to the relation

$$T_2 = 1/\pi\Delta\nu_{1/2} \quad (1)$$

The corresponding  $\tau$  values, the average time between diffusional jumps, were then obtained using the simplified Wolf<sup>17</sup> equation for a monovacancy diffusion mechanism in a body-centred cubic lattice:

$$1/T_2 = 1.40M_{2r}\tau \quad (2)$$

where  $M_{2r}$  is the rotationally averaged second moment. The mean value of  $M_{2r}$ , evaluated from low-field  $T_{1\rho}$  measurements<sup>7</sup> is  $3.11 \times 10^8 \text{ s}^{-2}$ . The  $\tau$  values have been deduced from the experimental linewidths using eqns. (1) and (2). The average time between diffusional jumps at the melting point  $\tau_m = 1.7 \times 10^{-7} \text{ s}$ . This value is at the extreme value of the range reported for body-centred cubic solids  $(1.2 \pm 0.6) \times 10^{-7} \text{ s}$ .<sup>1</sup> The more loosely packed body-centred cubic crystals are stable at relatively higher temperatures than the closer packed face-centred cubic structure. It has been reported<sup>18</sup> that the translational jump frequencies of disordered crystals at the melting point are characteristically a factor of five greater for body-centred cubic than for face-centred cubic solids, and independent of the degree of orientational disorder. The motionally averaged NMR resonances of body-centred cubic solids might therefore be narrower than for face-centred cubic solids. However, the NMR linewidths of HMDS are comparable to those observed for the disordered face-centred cubic solids of pivalic acid,<sup>19</sup> *tert*-butyl chloride<sup>20</sup> and *tert*-butyl bromide.<sup>10</sup>

The value of  $\tau$  is related to the self-diffusion coefficient  $D$  through the Einstein relationship

$$D = \langle r^2 \rangle / 6\tau \quad (3)$$

where  $\langle r^2 \rangle$  is the mean-square-jump distance which can be put equal to  $(3/4)a^2$  for a body-centred cubic lattice. The values of  $D$  deduced from the linewidth data are shown in Fig. 2.

We have also measured the self-diffusion coefficients in HMDS in the liquid and disordered phases using the PFG technique (Fig. 2). The corresponding activation en-

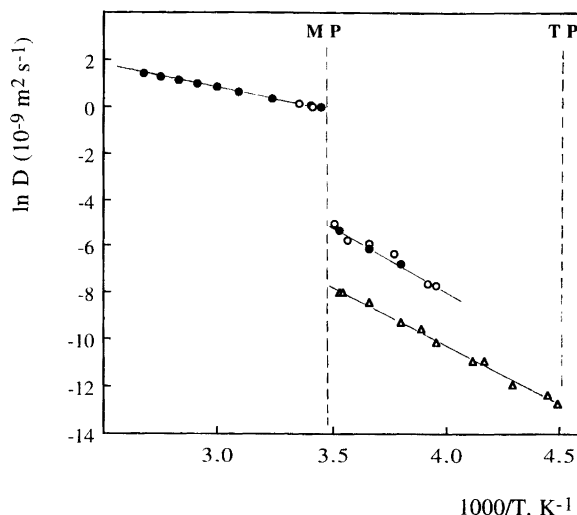


Fig. 2. Self-diffusion coefficients of HMDS versus reciprocal temperature:  $^1\text{H}$  and  $^{13}\text{C}$  PFG results at 200.13 MHz ( $\bullet$ ) and 100.62 MHz ( $\circ$ ), respectively;  $^1\text{H}$  linewidth results at 400.13 MHz ( $\Delta$ ).

ergies, obtained from linear regression, are 15 and 47 kJ mol<sup>-1</sup>, respectively. The self-diffusion measurements of solid I were carried out only in a limited temperature range (253–285 K) due to short  $T_2$  (13 ms at 253 K for  $^{13}\text{C}$ ) and limited field-gradient strength ( $\leq 0.86 \text{ T m}^{-1}$ ). The linear Arrhenius plots ( $\ln D$  against  $T^{-1}$ ) in Fig. 2 indicate that a single diffusion process is taking place in solid I. However, the PFG technique gives  $D$  values that are about an order of magnitude larger than the values obtained from the indirect linewidth method;  $D_m = 7.0 \times 10^{-12}$  and  $5.1 \times 10^{-13} \text{ m}^2 \text{ s}^{-1}$  at the melting point, respectively. These values are, however, in reasonable agreement with the value evaluated from the radiotracer measurements by Chadwick *et al.*<sup>7</sup> ( $6.5 \times 10^{-13} \text{ m}^2 \text{ s}^{-1}$ ) and fall within the range normally observed for disordered solids.<sup>1</sup> Linear regression on the linewidth data of Fig. 2 yielded an activation energy of 42 kJ mol<sup>-1</sup> compared to 47 kJ mol<sup>-1</sup> obtained from the PFG data. These activation energies are in fair agreement with the values obtained from  $T_{1\rho}$  measurements (44 kJ mol<sup>-1</sup>) and radiotracer measurements (52 kJ mol<sup>-1</sup>).<sup>7</sup> Contemporary  $T_{1\rho}$  measurements by Albert *et al.*,<sup>6</sup> however, produced a much smaller activation energy (36 kJ mol<sup>-1</sup>), whereas a subsequent plastic deformation and radiotracer investigation by Salthouse and Sherwood<sup>12</sup> yielded considerably larger values (68 and 71 kJ mol<sup>-1</sup>, respectively). The latter experiment measured, however, the diffusion of hexamethylethane- $^{14}\text{C}$  in HMDS. The serious discrepancies between the reported activation energies largely reflect the effect of impurity and the history of the sample as well as different measuring techniques. The radiotracer results may be influenced by impurity induced grain-boundaries.<sup>12</sup> NMR relaxation measurements, however, monitor molecular diffusion within the crystallites, and there is no serious systematic error due

to sample crystallinity. Moreover, PFG and radiotracer methods, unlike NMR relaxation, involve a long time-scale observation of the diffusion process. Finally, for low entropy of fusion solids ( $<2.5 R$ ), activation energies for the line-narrowing process are usually much lower than those of self-diffusion obtained from plastic deformation and radiotracer measurements.<sup>21</sup>

**Spin-lattice relaxation.** The  $^1\text{H}$ ,  $^2\text{H}$ ,  $^{13}\text{C}$  and  $^{29}\text{Si}$   $T_1$  values were measured for the liquid and solid phases of HMDS.  $^2\text{H}$  and  $^{29}\text{Si}$   $T_1$  values of solid II were not measured, however, owing to complex absorption profiles and/or poor signals. Semi-logarithmic plots of  $T_1$  versus inverse temperature are shown in Figs. 3–6. The large discontinuities in the  $^1\text{H}$  and  $^{13}\text{C}$   $T_1$  values at the transition point imply, as expected, that different motions dominate the spin-lattice relaxation in the two phases. The marked discontinuity in  $T_1$  of the investigated nuclei at the melting point, followed by a significant change in the activation energy, shows that the rate and possible type of reorientation are significantly affected by the melting process (*vide infra*).

**Solid II.** In this phase only internal  $\text{C}_3$  and  $\text{C}_3'$  reorientations with correlation times  $\tau_m$  and  $\tau_M$ , respectively, modulate the dipolar  $^1\text{H}$  and  $^{13}\text{C}$  relaxation. The negative slopes of the  $^1\text{H}$  and  $^{13}\text{C}$   $T_1$  curves in this phase imply that the extreme narrowing condition prevails. If only one motion dominates, the relevant relaxation rates are given by eqns. (4) and (5)<sup>9,10,19</sup>

$$\frac{1}{T_1(^1\text{H})} = \left(\frac{\mu_0}{4\pi}\right)^2 A\gamma_{\text{H}}^4 \hbar^2 (r_{\text{HH}}^{-6} + 3r_{\text{HH}'}^{-6}) \tau_i \quad (4)$$

$$\frac{1}{T_1(^{13}\text{C})} = \left(\frac{\mu_0}{4\pi}\right)^2 B\gamma_{\text{H}}^2 \gamma_{\text{C}}^2 \hbar^2 r_{\text{CH}}^{-6} \tau_i \quad (5)$$

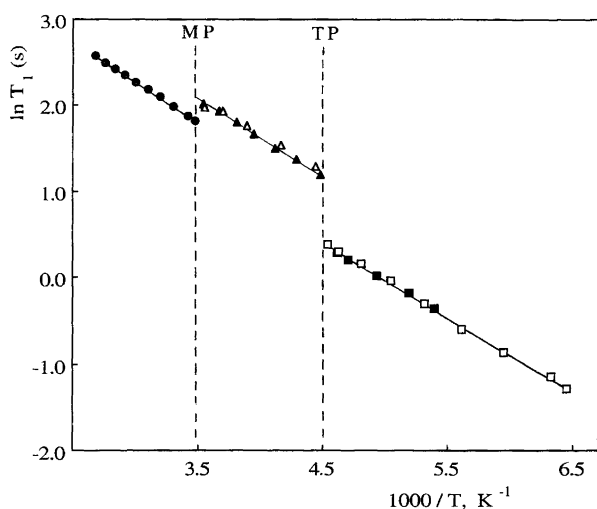


Fig. 3.  $^1\text{H}$   $T_1$  relaxation times of HMDS versus reciprocal temperature measured at 200.13 MHz (filled symbols) and 400.13 MHz (open symbols).

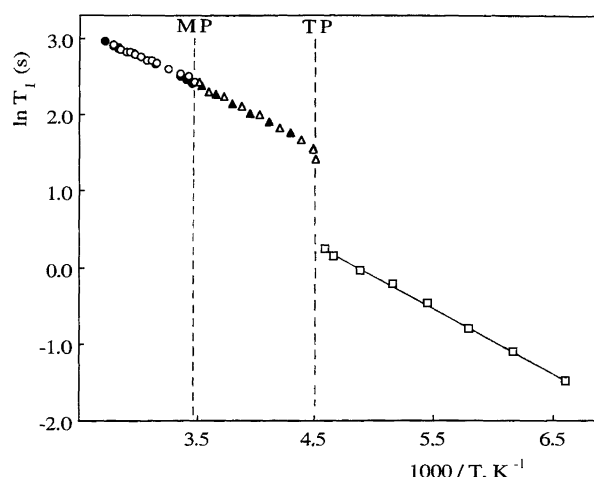


Fig. 4.  $^{13}\text{C}$   $T_1$  relaxation times of HMDS versus reciprocal temperature measured at 50.32 MHz (filled symbols) and 100.62 MHz (open symbols).

where  $\tau_i = \tau_M$  or  $\tau_m$  as appropriate,  $r_{\text{HH}}$  is the internuclear H–H separation within a  $\text{CH}_3$  group,  $r_{\text{HH}'}$  is the distance between the centres of the equilateral triangles formed by the three hydrogen atoms of each methyl group and  $r_{\text{CH}}$  is the C–H bond length. If all carbon and silicon atoms of HMDS have tetrahedral geometry  $A = 9/4$  for both motions (and not different as claimed by Albert *et al.*<sup>6</sup>), whereas  $B = 16/9$  for the  $\text{C}_3'$  motion and  $B = 32/27$  for the  $\text{C}_3$  motion. When evaluating eqn. (4) we have approximated the intra  $\text{CH}_3$ – $\text{CH}_3$  interactions by assuming that the protons in each  $\text{CH}_3$  group are located at the centre of the H–H–H triangle. As a consequence of this approximation  $\text{C}_3$  rotations will have no effect on the  $r_{\text{HH}'}$  vector and hence the  $3r_{\text{HH}'}$  term in eqn. (4), which should be skipped when the relaxation is governed by this motion. The C–H and Si–C bond lengths ( $r_{\text{CH}}$  and  $r_{\text{SiC}}$ ) are assumed to be 0.110 and 0.188 nm,<sup>22</sup> giving  $r_{\text{HH}} = 0.180$  nm and  $r_{\text{HH}'} = 0.367$  nm, respectively. It is then readily calculated that the intra  $\text{CH}_3$ – $\text{CH}_3$  interactions modulated by the  $\text{C}_3'$  motion only contribute 4% to the relaxation rate.

A minimum in  $T_1(^1\text{H})$  at 25 MHz is observed around 87 K.<sup>6</sup> Although this minimum is shifted towards higher temperatures at high field it is not observed within the investigated temperature range (155–220 K) of solid II (Fig. 3). This observation is consistent with the negative slopes of the  $^1\text{H}$  and  $^{13}\text{C}$   $T_1$  curves, showing that all  $T_1$  values are on the high-temperature side of the minimum. By using linear regression on the  $^1\text{H}$  and  $^{13}\text{C}$   $T_1$  data of Figs. 3 and 4 activation energies of 7.1 and 7.0  $\text{kJ mol}^{-1}$  were obtained, respectively, in good agreement with the early result of Albert *et al.*<sup>6</sup> (6.5  $\text{kJ mol}^{-1}$ ) but inconsistent with the value reported by Chadwick *et al.*<sup>7</sup> (9.2  $\text{kJ mol}^{-1}$ ). The latter value was, however, obtained from a very short linear range of the Arrhenius plot. This activation energy must be assigned either to the methyl rotation ( $\text{C}_3$  motion) or the rotation about the Si–Si axis ( $\text{C}_3'$  motion). We have thus calculated the corresponding

correlation times using eqns. (4) and (5). The best agreement between the  $^1\text{H}$  and  $^{13}\text{C}$  data is obtained for the  $\text{C}_3'$  motion in opposition to the assignment made on basis of the early  $^1\text{H}$  low-field data.<sup>6,7</sup> As pointed out in the introduction, however, it is not possible to distinguish between  $\text{C}_3$  and  $\text{C}_3'$  motions using only  $^1\text{H}$  data. The relatively low activation energy observed for the low-temperature motion of HMDS compared to hexamethylethane<sup>6,23</sup> and other *tert*-butyl compounds<sup>10,20,24,25</sup> (12–15  $\text{kJ mol}^{-1}$ ) probably reflects reduced interactions between the  $\text{Si}(\text{CH}_3)_3$  groups, in contrast to the *tert*-butyl groups, on different ends of the molecule owing to longer bonds. On the other hand, one might argue that the longer bonds in HMDS as compared to hexamethylethane will reduce the interactions between the methyl groups, and hence also cause a reduction in the activation energy of the  $\text{C}_3$  rotation.<sup>6</sup>

A maximum is observed for  $T_1(^1\text{H})$  at low field owing to the onset of the  $\text{C}_3$  motion (or alternatively  $\text{C}_3'$  motion) with activation energy 30–31  $\text{kJ mol}^{-1}$ .<sup>6,7</sup> Since the maximum is shifted to higher temperatures with increasing field strength, it is not observed at 200 and 400 MHz before the melting process intervenes.

*Liquid and solid I.* The dipolar and quadrupolar  $^1\text{H}$ ,  $^{13}\text{C}$  and  $^2\text{H}$  spin–lattice relaxations in these phases are governed by the overall tumbling motion as well as internal  $\text{C}_3$  and  $\text{C}_3'$  reorientations. The negative slopes of the  $T_1$  curves in the liquid and disordered phases imply that the extreme narrowing condition prevails. The relevant relaxation rates are therefore given by eqns. (6)–(8)<sup>19</sup>

$$\frac{1}{T_1(^1\text{H})} = \left(\frac{\mu_0}{4\pi}\right)^2 3\gamma_{\text{H}}^4 \hbar^2 (r_{\text{HH}}^{-6} \tau_{\text{eff}}^{\text{HH}} + 3r_{\text{HH}'}^{-6} \tau_{\text{eff}}^{\text{HH}'}) \quad (6)$$

$$\frac{1}{T_1(^{13}\text{C})} = \left(\frac{\mu_0}{4\pi}\right)^2 3\gamma_{\text{H}}^2 \gamma_{\text{C}}^2 \hbar^2 r_{\text{CH}}^{-6} \tau_{\text{eff}}^{\text{CH}} \quad (7)$$

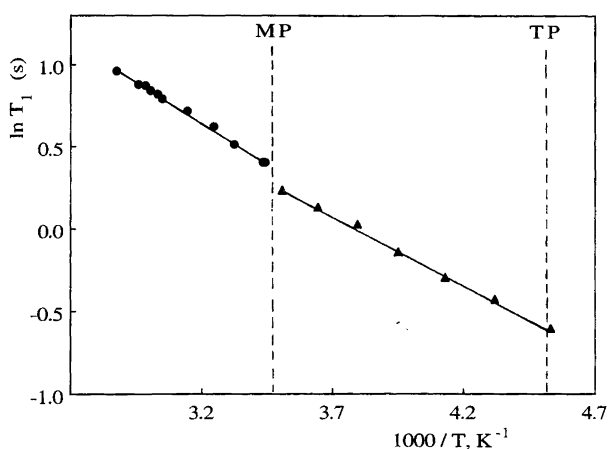


Fig. 5.  $^2\text{H}$   $T_1$  relaxation times of HMDS versus reciprocal temperature measured at 61.42 MHz.

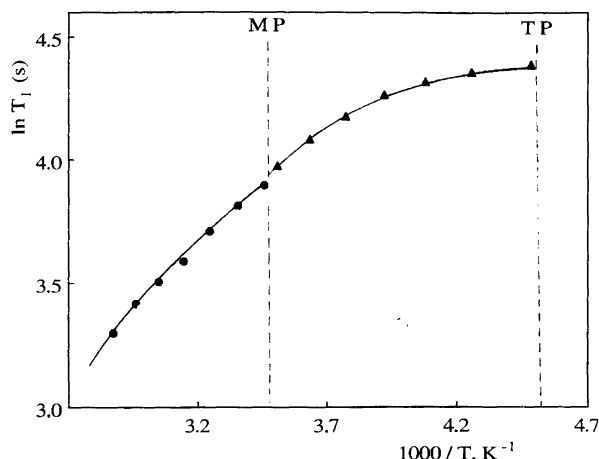


Fig. 6.  $^{29}\text{Si}$   $T_1$  relaxation times of HMDS versus reciprocal temperature measured at 79.50 MHz.

$$\frac{1}{T_1(^2\text{H})} = \frac{3}{2} \pi^2 \chi^2 \tau_{\text{eff}}^{\text{CH}} \quad (8)$$

where  $\chi = e^2 q Q / h$  is the quadrupolar coupling constant and the  $\tau_{\text{eff}}$  terms in eqns. (6)–(8), the so-called effective correlation times, are functions of the correlation times of the contributing motions.<sup>19</sup> Since the contribution from the  $3r_{\text{HH}'}^{-6}$  term in eqn. (6) is small (ca. 4%), we can make the approximation that  $\tau_{\text{eff}}^{\text{HH}'} = \tau_{\text{eff}}^{\text{HH}}$ .

A knowledge of the quadrupolar coupling constant of the  $\text{CH}_2^2\text{H}$  group is necessary in order to calculate the correlation times from the observed  $T_1(^2\text{H})$  values with eqn. (8).  $\chi$  Values of 180 and 191 kHz have been obtained for the liquid and solid phases, respectively, by substituting the  $T_1(^{13}\text{C})$  and  $T_1(^2\text{H})$  values at the melting point, obtained from linear regression, into eqns. (7) and (8). These values are somewhat larger than those reported for *tert*-butyl compounds (163–174 kHz)<sup>19,24,25</sup> but well within the range found for  $\text{C}^2\text{H}$  groups (150–250 kHz).<sup>26</sup>

The  $^1\text{H}$ ,  $^{13}\text{C}$  and  $^2\text{H}$   $T_1$  data of solid I yield practically identical activation energies of 7.0, 7.1 and 6.9  $\text{kJ mol}^{-1}$ , respectively. The previously reported activation energy ( $\geq 6.3 \text{ kJ mol}^{-1}$ )<sup>6,7</sup> is not accurate, since an increasing contribution from intermolecular relaxation, modulated by translational diffusion, resulted in a non-linear  $\ln T_1$  against  $T^{-1}$  plot. The effective correlation times at the melting point deduced from the  $^1\text{H}$  and  $^{13}\text{C}$   $T_1$  values, are also quite similar (2.4 and 1.4 ps, respectively) and well within the range reported for a series of related *tert*-butyl compounds (0.9–4.2 ps).<sup>10,20,24,25</sup> The comparable activation energies and rotational correlation times obtained from the appropriate interaction vectors of the  $^1\text{H}$ ,  $^{13}\text{C}$  and  $^2\text{H}$  nuclei suggest that the spin–lattice relaxation is dominated by near-isotropic overall tumbling in solid I.

The marked decrease in  $E_a$  for the  $^{13}\text{C}$ – $^1\text{H}$  vector, from 7.1  $\text{kJ mol}^{-1}$  in solid I to 5.8  $\text{kJ mol}^{-1}$  in the liquid, presumably reflects an increasing contribution from the spin–rotation mechanism. By contrast, the activation en-

ergies obtained from the  $T_1(^1\text{H})$  and  $T_1(^2\text{H})$  data increase by 0.9 and 1.4 kJ mol<sup>-1</sup>, respectively, when going from solid I to the liquid state, followed by a slight increase in  $\tau_{\text{eff}}^{\text{HH}}$  on melting. These results indicate, in accord with previous observations,<sup>10,20,24,25</sup> that the molecular reorientations are slightly retarded by the melting process.

The temperature behaviour of the  $T_1(^{29}\text{Si})$  values is the opposite of that seen for the other nuclei, i.e.  $T_1$  decreases with increasing temperature in both the liquid and solid I phases. This behaviour is attributed to a self-diffusion dominated relaxation mechanism with  $\omega_{\text{Si}}\tau \gg 1$ , where  $\tau$  is the average time between diffusional jumps. Indeed, by using the value of  $\tau$  at the melting point of solid I,  $1.7 \times 10^{-7}$  s, deduced from the linewidth data, it follows that  $\omega_{\text{Si}}\tau = 85$ . However, the non-linear  $T_1$  curve seen in Fig. 6 implies that the intramolecular dipole-dipole interactions, modulated by molecular reorientations, make a significant contribution to the relaxation in solid I. Indeed, the observation that  $T_1(^{29}\text{Si})$  is approaching a maximum near the phase transition point shows that the latter mechanism is becoming the more important relaxation mechanism when the phase transition intervenes.  $T_1(^{29}\text{Si})$  is, by contrast, dominated by self-diffusion modulated relaxation at the high-temperature region of the liquid state. In fact, the three  $T_1$  values at highest temperature yield an activation energy of ca. 15 kJ mol<sup>-1</sup>, in excellent agreement with the value obtained from the self-diffusion measurements.

## References

- Sherwood, J. N. *The Plastically Crystalline State*, Wiley, New York 1979.
- Parsonage, N. G. and Staveley, L. A. K. *Disorder in Crystals*, Clarendon Press, Oxford 1978.
- Suga, H. and Seki, S. *Bull. Chem. Soc. Jpn.* 32 (1959) 1088.
- Amoureux, J. P., Foulon, M., Muller, M. and Bee, M. *Acta Cryst., Sect. B* 42 (1986) 78.
- Yukitoshi, T., Suga, H., Seki, S. and Itoh, J. *J. Phys. Soc. Jpn.* 12 (1957) 506.
- Albert, S., Gutowsky, H. S. and Ripmeester, J. A. *J. Chem. Phys.* 56 (1972) 1332.
- Chadwick, A. V., Chezeau, J. M., Folland, R., Forrest, J. W. and Strange, J. H. *J. Chem. Soc. Faraday Trans. 1* (1975) 1610.
- Ripmeester, J. A. and Ratcliffe, C. I. *J. Chem. Phys.* 82 (1985) 1053.
- Albert, S., Gutowsky, H. S. and Ripmeester, J. A. *J. Chem. Phys.* 64 (1976) 3277.
- Aksnes, D. W., Ramstad, K. and Bjørlykke, O. P. *Magn. Reson. Chem.* 25 (1987) 1063.
- Folland, R., Ross, S. M. and Strange, J. H. *Mol. Phys.* 26 (1973) 27.
- Salthouse, P. W. and Sherwood, J. N. *J. Chem. Soc. Faraday Trans. 1* (1977) 1845.
- Lohmann, J. A. B. *Personal communication*, 1992, Bruker Spectrospin Ltd., Banner Lane, Coventry CV4 9GH, UK.
- Longworth, L. G. *J. Phys. Chem.* 64 (1960) 1914.
- Callaghan, P. T. *Principles of Nuclear Magnetic Resonance Microscopy*, Clarendon Press, Oxford 1993.
- Garroway, A. N. *J. Magn. Reson.* 28 (1977) 365.
- Wolf, D. *Phys. Rev., Sect. B* 10 (1974) 2710.
- Boden, N. *Chem. Phys. Lett.* 46 (1977) 141.
- Aksnes, D. W. and Kimtys, L. L. *Magn. Reson. Chem.* 28 (1990) S20.
- Aksnes, D. W. and Ramstad, K. *Magn. Reson. Chem.* 26 (1988) 1086.
- Bladon, P., Lockhart, N. C. and Sherwood, J. N. *Mol. Phys.* 20 (1971) 577.
- Huggins, M. L. *J. Am. Chem. Soc.* 75 (1953) 4123.
- Chezeau, J. M., Dufourcq, J. and Strange, J. H. *Mol. Phys.* 20 (1971) 305.
- Mooibroek, S., Wasylshen, R. E., MacDonald, J.B., Ratcliffe, C. I. and Ripmeester, J. A. *Can. J. Chem.* 66 (1988) 734.
- Mooibroek, S. and Wasylshen, R. E. *Can. J. Chem.* 63 (1985) 2926.
- Mantsch, H. H., Saito, H. and Smith, I. C. P. In Emsley, J. W., Feeney, J. and Sutcliffe, L. H., Eds., *Progr. Nucl. Magn. Reson. Spectrosc.*, Vol. 11, p. 211, Pergamon Press, Oxford 1977.

Received January 20, 1995.